Suppressing and enhancing effects of mesoscale dynamics on biological production in the Mozambique Channel

Y.S. José[a,b,*], P. Penven[b,c], O. Aumont[d], E. Machu[c], C.L. Moloney[e], F. Shillington[b], O. Maury[f,g]

[a] Helmholtz Centre for Ocean Research Kiel, Germany
[b] Department of Oceanography, Marine Research Institute (Ma-Re), University of Cape Town, South Africa
[c] Laboratoire de Physique des Océans(UMR 6523 CNRS, Ifremer, IRD, UBO), France
[d] Laboratoire d'Océanographie et du Climat: Expérimentations et Approches Numériques (UMR 7159 CNRS, UPMC, IRD, MNHN), France
[e] Department of Biological Sciences, Marine Research Institute (Ma-Re), University of Cape Town, South Africa
[f] Institut de Recherche pour le Développement - UMR 248 MARBEC, France
[g] International Laboratory ICEMASA, Department of Oceanography, University of Cape Town, South Africa

ARTICLE INFO

ABSTRACT

We used a coupled physical–biogeochemical model to investigate how the strong eddy activity typical of the Mozambique Channel affects biological production. A numerical experiment was carried out, in which mesoscale dynamics were suppressed by cancelling the nonlinear terms for horizontal momentum in the Naviers–Stokes equation.

Mesoscale dynamics were found to be responsible for (1) increased offshore production in the Mozambique Channel as a result of net eddy-induced offshore transport of nutrient-rich coastal waters; (2) decreased shelf production along the central Mozambican and south-west Madagascar coast caused by a reduction in nutrient availability related to the net eddy-induced lateral transport of nutrients; (3) increased coastal production along the northern Mozambican coast caused by eddy-induced nutrient supply.

The model results also showed an intensification and shallowing of the subsurface production, related to increased upper layer nutrient concentrations caused by eddy activity.

In addition, by driving the detachment of the East Madagascar Current at the southern tip of the island, inertial processes intensify the southern Madagascar upwelling and causes offshore diffusion of the upwelled waters.

These results emphasize the complex role played by eddy activity and, more generally, inertial processes on marine ecosystems in this region.

1. Introduction

By supplying nutrient-rich waters to the near surface layer which is depleted in nutrients, mesoscale eddies are known to play a key role in the stimulation of biological production (McGillicuddy et al., 1998; Oschlies and Garçon, 1998; Williams and Follows, 1998; Lévy et al., 2001). This nutrient supply is primarily exercised through vertical pumping from subsurface nutrient-rich layers (McGillicuddy et al., 1998; Oschlies and Garçon, 1998; Lévy et al., 2001) and lateral transport from nutrient-rich waters to low nutrient environments (Williams and Follows, 1998). This conventional view of

eddies stimulating biological production was recently found inadequate in eastern boundary upwelling systems (Lathuilière et al., 2010; Gruber et al., 2011). Using both observational and model simulated dynamics, Gruber et al. (2011) showed that eddy activity exerts a suppressive effect on coastal biological production in coastal upwelling systems.

This reduction in coastal production was related to the eddy-induced intensification of lateral transport of coastal productive waters toward offshore regions (Gruber et al., 2011). This came in support of a study by Lathuilière et al. (2010), in which using an idealized circulation model of a coastal upwelling, the authors found a reduction of coastal production due to mesoscale variability. This finding raises the question of whether a reducing effect of eddy stirring on coastal production could also occur in regions with much stronger eddy activity. The present study aims to investigate the impact of mesoscale eddies on biological production in the Mozam-

bique Channel, a region characterized by intense eddy activity, with a particular focus on the effect of eddy dynamics on coastal production.

The Mozambique Channel is a western boundary current system, where the eddy activity is among the strongest in the world (Chelton et al., 2007). The ocean circulation of the Mozambique Channel is dominated by large anticyclonic rings, which propagate southward through the Channel (Saetre and Silva, 1984; Grundlingh, 1995; de Ruijter et al., 2002; Schouten et al., 2003; Halo et al., 2014). These eddies are often in strong interaction with the continental shelf and the coastal regions (de Ruijter et al., 2002; Ternon et al., 2014; José et al., 2014). These eddy-shelf interactions result in offshore entrainment of coastal productive waters (Quartly and Srokosz, 2003; José et al., 2014; Lebourges-Dhaussy et al., 2014).

In this study, we used a coupled physical–biogeochemical model developed by José et al. (2014) to simulate realistically the dynamics of the Mozambique Channel. After validating the simulated dynamics against the observed data, we ran an idealized experiment in which we removed the terms responsible for the occurrence of eddies. This was performed by canceling the advection of momentum, all the other terms and parameters being kept strictly the same. Gruber et al. (2011) have used the same method for testing the role of eddies on biological production in the California Current System. As described by Gruber et al. (2011), the advantage of this method over the coarsening of the horizontal resolution is a better preservation of large scale Ekman and geostrophic circulations. By using the method in which the advection of momentum are cancelled, we investigate the effects of mesoscale dynamics on biological production without including other potential sources of differences.

By comparing the realistic simulation with the idealized experiment, we demonstrate that the role of eddy activity on coastal production is complex, with both reducing and increasing coastal production, depending on the location.

2. Material and methods

The physical–biogeochemical model configuration used for the Mozambique Channel consists of a hydrodynamic model ROMS (Regional Ocean Modelling System) coupled with a biogeochemical model PISCES (Pelagic Interaction Scheme for Carbon and Ecosystem Studies). This configuration is based on the ROMS_AGRIF two-way embedding procedure (Debreu et al., 2008, 2012) to nest a high resolution regional domain (child grid) within a larger scale domain (parent grid). ROMS is a split-explicit, free surface, terrain-following vertical coordinates ocean model, which solves the primitive equations of Navier Stokes in the presence of rotation (Shchepetkin and McWilliams, 2005). PISCES is a biogeochemical model that simulates the first trophic levels of the marine ecosystem and the biogeochemical cycles of carbon and the main nutrients (Aumont and Bopp, 2006). The PISCES parameterizations are described in detail in Aumont and Bopp (2006). This model has 24 compartments, of which four are living pools composed of two phytoplankton size-classes (nanophytoplankton and diatoms) and two zooplankton size-classes (microzooplankton and mesozooplankton). It incorporates phytoplankton growth limitation by five external nutrients: nitrate, ammonium, phosphate, silicate and iron. The Mozambique Channel configuration, described in detail by José et al. (2014), consists of a parent domain at $1/2°$ horizontal resolution, covering the south-western Indian ocean, while the child grid domain at $1/6°$ resolution extends from $32°S$ to $1.5°S$ and from $28°E$ to $61°E$. In this region characterized by a first baroclinic Rossby radius of deformation ranging from 50 to 100 km (Chelton et al., 1998), a resolution of $1/6°$ resolves most of the spectrum of mesoscale eddies. This is confirmed by the level of mean eddy kinetic energy in Fig. 1. The surface forcing fields consist of monthly climatologies presented by Penven et al. (2008) and atmospheric dust deposition from Fung and Tegen (1995). Due

to the absence of reliable data on river nutrient discharges in this region, river inputs are not included in this configuration. Initial and boundary conditions for all the prognostic variables are derived from a monthly climatology of a NEMO/PISCES model simulation of the Indian Ocean (Koné et al., 2009). This realistic ROMS configuration is used as a reference and is referred to as REF.

To quantify the impact of mesoscale dynamics on biological production, we have performed an experiment in which the mesoscale dynamics were suppressed (NoADV). To do so, we have cancelled the nonlinear advection terms in the Navier–Stokes equations for horizontal momentum. The cancellation of advection of momentum can be seen as a linearization for a low Rossby number, if we suppose that the eddies have neglectable upscaling effects on the large scale circulation. The absence of advection of momentum prevents the occurrence of coherent structures such as eddies and non linear cascades of energy (Yeung and Brasseur, 1991; Zhou, 1993; Eyink and Sreenivasan, 2006). This method is similar to the one described by Gruber et al. (2011) for their "non-eddy" simulation.

With the cancellation of these terms, we expect a suppression of eddies in the NoADV simulation, while the mean large scale circulation should be mostly preserved (since it follows linear Sverdrup dynamics).

Both simulations were run for a period of twenty climatological years, in which the model showed stable conditions after six years of simulation. Thus, the model outputs analyzed in this study were built by averaging, over the last ten years, the simulated fields of the high resolution child grid.

An extensive model–data comparison has been conducted using in situ climatologies and satellite products (José, 2014; José et al., 2014). It shows that the model is able to reproduce the mean state, seasonal cycle and eddy variability for physical and biogeochemical variables in the Mozambique Channel.

3. Results

3.1. Ocean circulation in the Mozambique Channel

The surface mean eddy kinetic energy (EKE), sea surface height (representing the surface circulation and surface elevation) and the mean sea surface currents from both simulations and AVISO altimetry products for the period 1993 to 2012 (produced by Ssalto/Duacs and distributed by Aviso, with support from Cnes —http://www.aviso.altimetry.fr/) are presented in Fig. 1. The simulated EKE from REF exhibits patterns consistent with AVISO altimetry (Fig. 1a,b), with values exceeding $1400 \text{ cm}^2 \cdot \text{s}^{-2}$ in the central Mozambique Channel. By cancelling the advection of momentum in NoADV, EKE decreased to below $100 \text{ cm}^2 \cdot \text{s}^{-2}$ in the Channel (Fig. 1c). The modeled sea surface height and surface currents for early December of model year 20 show an absence of eddy structures in NoADV, while in REF, anticyclonic and cyclonic eddies are present in the Channel (Fig. 1d,e). This confirms that cancelling the advection of momentum succeeds in the removal of Mozambique Channel eddies. The remaining EKE in the northern part of the domain in NoADV could be related to Rossby waves propagating from the east, resulting in variations in the NMC (Schouten et al., 2003). The remain EKE further east could be related to waves generated on the Mascarene plateau (New et al., 2013).

The intensity of the observed and simulated geostrophic currents suggests that the REF simulation captures the strength of the surface currents of the south-western Indian ocean system, relevant to the circulation in the Mozambique Channel (Fig. 1f,g). However, the magnitude of the simulated North Madagascar current (NMC, around $100 \text{ cm} \cdot \text{s}^{-1}$) is higher compared to AVISO altimetry (around $50 \text{ cm} \cdot \text{s}^{-1}$), but is consistent with in situ observations presented by Schott and McCreary (2001). The flow along the northern Mozambican Channel coast is consistent with the observed
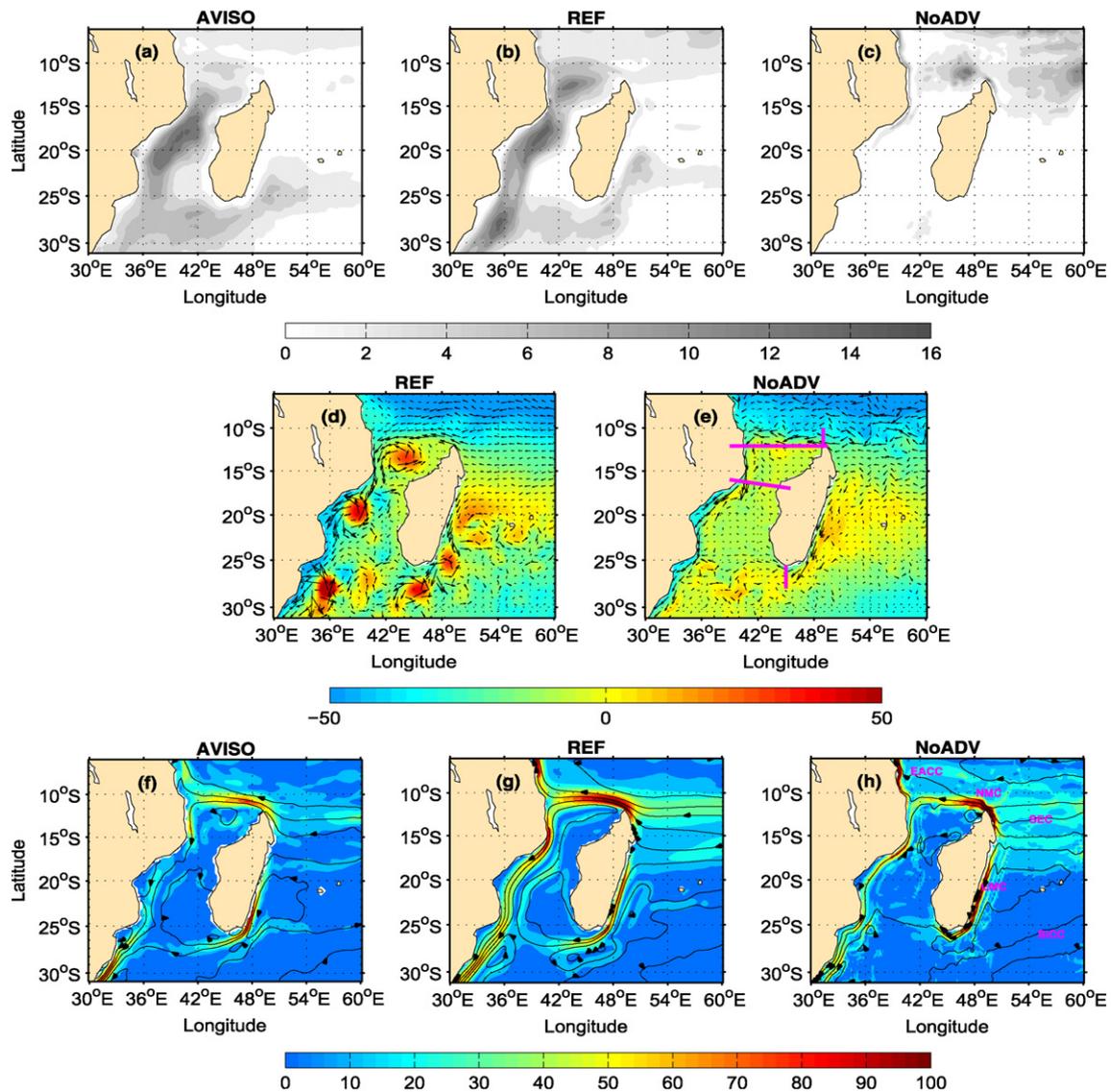
Fig. 1. Sea surface physical dynamics of the south western Indian ocean. (a–c) eddy kinetic energy [$10^2 \times cm^2\ s^{-2}$], (d,e) sea surface currents (arrows) overlaid on sea surface anomaly [cm] for early December of model year 20 and (f–h) sea surface height [contour every 10 cm] overlayed on the current intensity [$cm \cdot s^{-1}$]. Variables corresponding to *AVISO* observations (a,f), *REF* simulation (b,d,g) and *NoADV* experiment (c,e,h). Magenta lines in panel (e) show the location of the vertical sections displayed on Fig. 2.

field of Saetre (1985) and shows southward currents with intensity up to 75 cm·s⁻¹. These results emphasize the underestimation of the magnitude of the surface currents by *AVISO* altimetry products (Ternon et al., 2014). By comparing *AVISO* and the *in situ* measured surface circulation, Ternon et al. (2014) found an underestimation of about 30% in altimetry observations compared to *ADCP* measurements and of about 20% compared to drifters.

Cancelling the advection of momentum did not, in contrast, significantly alter the major patterns of the large scale circulation of this region (contours in Fig. 1h). Both *REF* (Fig. 1g) and *NoADV* (Fig. 1h) reproduce the observed large scale mean surface patterns, showing the South Equatorial Current (*SEC*) flowing westward and its bifurcation east of Madagascar (Schott and McCreary, 2001; Schott et al., 2002; Palastanga et al., 2006, 2007). The north-going branch of the *SEC*, the *NMC*, appears closer inshore and more intensified in *NoADV* than in *REF* and *AVISO*. Further west, the *NMC* splits into two branches: the East Africa Coastal Current *EACC* and the southward mean transport through the Mozambique Channel. Inside the

Mozambique Channel, the mean local surface circulation is modified by the absence of mesoscale eddies. The flow through the Channel is predominantly southward and weaker in *NoADV* than in *REF* and *AVISO*. This weaker flow in *NoADV* illustrates the rectification effects of Mozambique Channel eddies on the mean circulation pattern of the Channel. In contrast to *NoADV*, the *REF* and *AVISO* surface circulations present a northward flow in the middle of the Channel, adjacent to a southward flow, consistent with the passage of anticyclonic Mozambique Channel rings.

The southward-going branch emanating from the split of the SEC, the East Madagascar Current (*EMC*), propagates along the east coast of Madagascar. South of Madagascar, the *EMC* hugs the shelf break in *NoADV* (Fig. 1h) while in *REF* (Fig. 1g) and *AVISO* (Fig. 1f) it detaches from the topography at the southern tip of Madagascar. Surprisingly, there is still a retroflecting loop in the mean *EMC* and the South Indian Counter Current (*SICC*) is present, despite the absence of advection of momentum in *NoADV*. However, this loop occurs earlier in comparison to what is simulated in *REF*. This retroflection
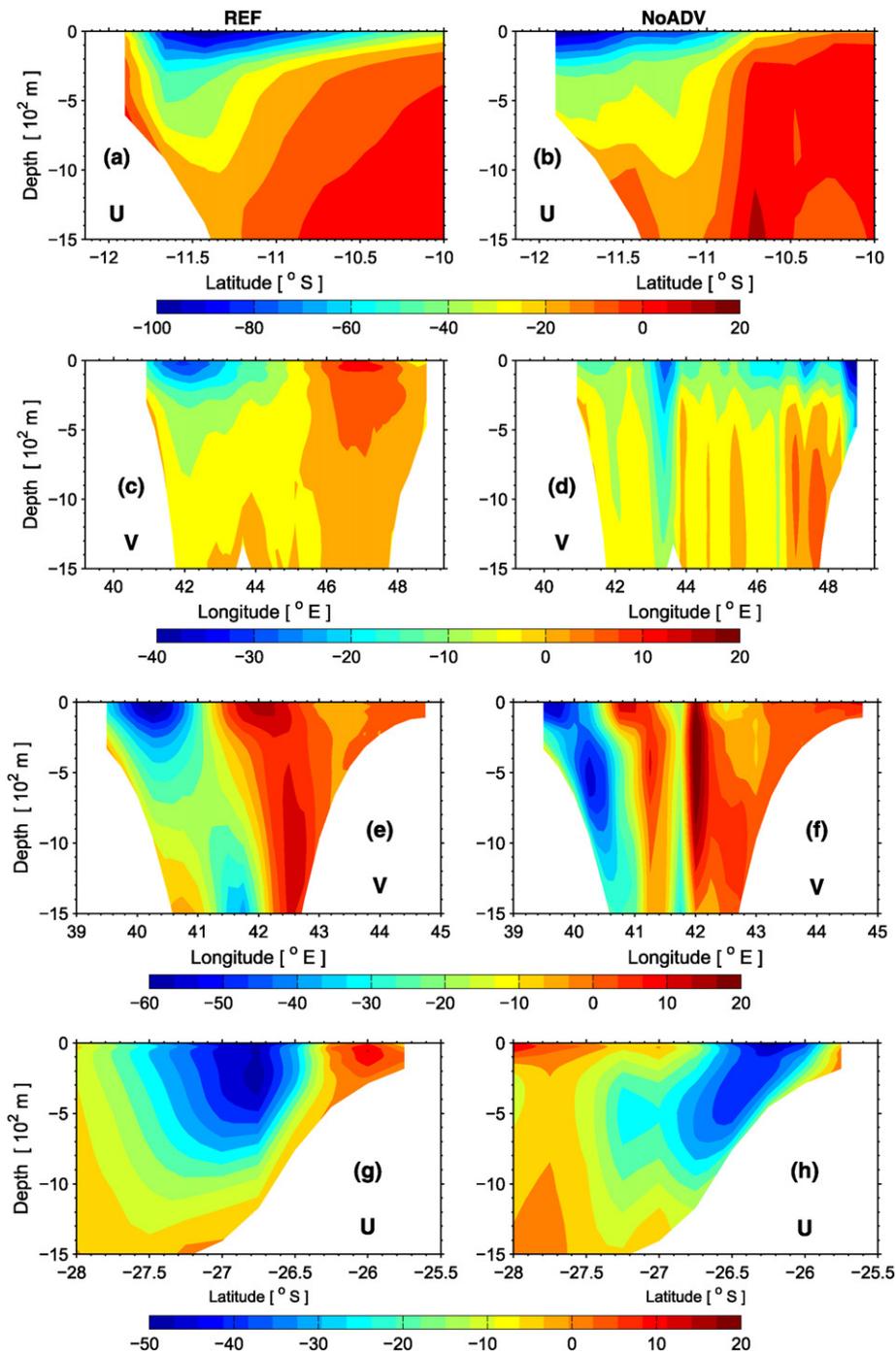
Fig. 2. Vertical structure of the mean velocity [cm • s^{-1}]. (a,b) Zonal velocity (U) at the northern tip of Madagascar, around 49°E. (c,d) Meridional velocity (V) at the northern border of the Mozambique Channel, around 12°S. (e,f) Meridional velocity (V) at the narrowest part of the Mozambique Channel, around 17°S. (g,h) Zonal velocity (U) at the southern tip of Madagascar, 45°E. Model results corresponding to *REF* (left panels) and *NoADV* (right panels). The locations of the sections are presented on Fig. 1e.

was previously related to the eddy activity generated in the southern tip of Madagascar by the detachment of the *EMC* from the coast (Grundlingh et al., 1991). The *NoADV* experiment also highlights the role of south Madagascar dipole eddies (de Ruijter et al., 2004) on the northward intrusion of water from the south into the Mozambique Channel. *REF* and *AVISO* show a cyclonic loop in the south east part of the Channel which is not represented in *NoADV*, where the flow is dominantly westward towards the African coast. This cyclonic loop could be related to a rectification effect due to the presence of cyclonic eddies generated south of Madagascar.

The suppression of mesoscale dynamics in *NoADV* reveals significant alterations in the current intensity and structure of the Mozambique Channel circulation related to eddy activity (Fig. 1g,h). North of Madagascar, the *NMC* appears intensified and confined inshore in *NoADV* (Fig. 1h). Conversely, the following westward flow toward the African coast appears weaker in this simulation. In *REF*, the core of the *NMC* appears slightly detached from the shelf in the northern tip of Madagascar, allowing the generation of an eastward circulation inshore (around 12°S and 49°E, Fig. 1g, Fig. 2a,b). This inshore eastward circulation has been related to the friction on the inshore edge
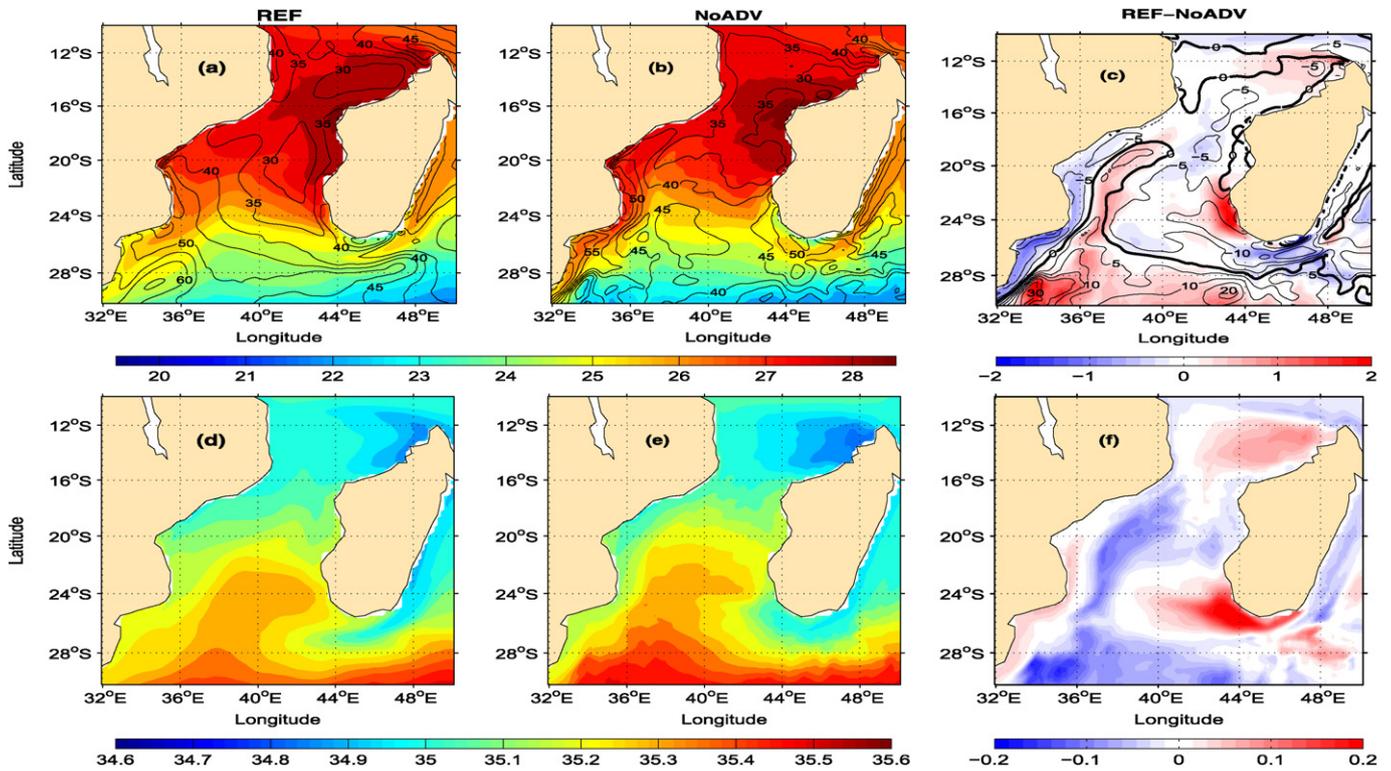
Fig. 3. Mean mixed layer depth [m] overlaid on mean sea surface temperature ([°], a–c) and mean salinity (d–f), corresponding to *REF* (left panels), *NoADV* (middle column) and the *REF–NoADV* anomalies (right panels).

of the *NMC*, which generates anticyclonic eddies that propagate into the Mozambique Channel (Backeberg and Reason, 2010). Reaching the northern Mozambique Channel, the anticyclonic eddies intensify and structure the flow through the Channel, with a southward flow along the western part and a northward flow along the eastern part of the Channel (Fig. 1g,h and 2c,d). This anticyclonic mean recirculation characteristic of the northern part of the Mozambique Channel is simulated in *REF* (Fig. 1g) but is not present in *NoADV* (Fig. 1h). This supports the findings of Collins et al. (2014), who related this recirculation to Mozambique Channel eddies. At the narrowest section of the Channel, around 17°S, the southward flow along the African coast is extended offshore and is surface intensified in *REF* (Fig. 2e,f), in agreement with *in situ* observed patterns (Ullgren et al., 2012). At the eastern Madagascar coast, the removal of mesoscale dynamics in *NoADV* did not affect the *EMC* (Fig. 1g,h). Downstream, at the southern tip of the island, the *EMC* appears attached to the coast, intensifying the coastal current (Fig. 1g,h and Fig. 2g,h). In contrast to *NoADV*, the detachment of the *EMC* from the shelf break in the *REF* allows an eastward flow onshore (Fig. 2g,h), triggering the formation of dipole eddies south of Madagascar (Fig. 2g,h, de Ruijter et al. (2004); Siedler et al. (2009)).

The impact of eddy activity in the Mozambique Channel is also evident from surface temperature and salinity (Fig. 3). In the northern part of the Mozambique Channel, the surface waters are slightly colder and fresher in *NoADV* (Fig. 3b,e). These changes seem to be related to the absence of the anticyclonic recirculation in *NoADV*. With the anticyclonic recirculation in *REF*, warmer waters on the central and northeastern side of the Mozambique Channel are diffused through the northern basin by the northward current present in the eastern Channel, increasing surface temperature (Fig. 3a–c). A similar pattern is observed for salinity (Fig. 3d–f). Similarly, saltier waters from the south are transported northward by the equatorward jet of the anticyclonic recirculation and are mixed with fresher

surface water from the north-east, increasing salinity. Futher south inside the Channel, the warm and fresh Tropical Surface Water (*TSW*), which propagates southward as a western boundary current, is closer to the shelf in *NoADV*. In this case, a sharp density front separates the warmer and fresher water along the western boundary from the colder and saltier water offshore. With the presence of Mozambique Channel eddies, water mass properties are mixed and the horizontal density gradient is reduced. This way, temperature is increased and salt content is reduced along the coast. Offshore, eddy turbulent diffusion induces an increase in temperature and a decrease in salinity. South of Madagascar, detachment of the *EMC* from the coast in *REF* transports the warmer and fresher *TSW* offshore. In addition, the cyclonic loop observed along the west Channel in *REF* brings southward warm and fresher waters from the central Mozambique Channel. Changes in water density induce changes in the mixed layer depth *MLD*. In the northern Channel, the *MLD* is deeper in the west basin in *REF*. This suggests that heat and salt redistribution by the Mozambique Channel eddies deepen the *MLD* in the west side of the basin. Further south, the *MLD* is dominantly shallower in *REF* compared to *NoADV*. An exception is observed offshore, coinciding with the region of horizontal density gradient in *NoADV*. This suggests that the mixing induced by eddy activity in this region deepens the *MLD*.

3.2. Plankton and nutrient dynamics

The seasonal cycles of sea surface chlorophyll for both *SeaWiFS* remote sensing observations and *REF* are presented in Fig. 4. The simulated chlorophyll concentrations follow the variability of the observations. They show lower concentrations during austral summer (Fig. 4a,c) and higher concentrations during austral winter (Fig. 4b,d). This variability is related to seasonal changes in the upper
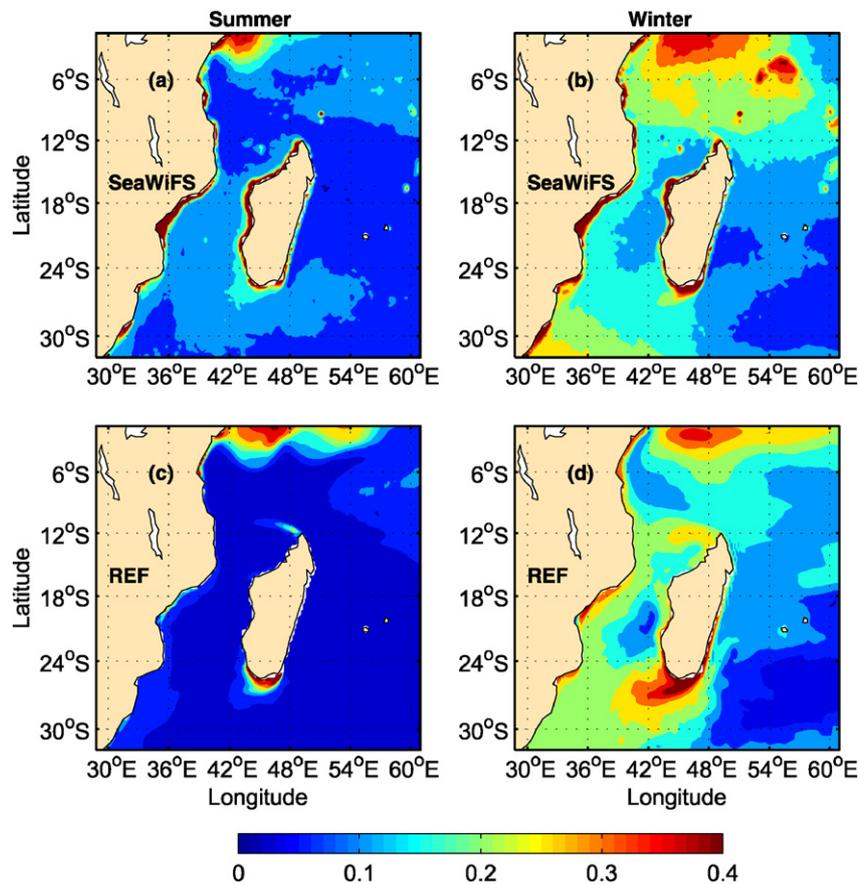
Fig. 4. Seasonal variability of sea surface chlorophyll [mg · m^{-3}], corresponding to *SeaWiFS* observations (a,b) and *REF* simulation (c,d). The high production occurs in austral winter season (right panels) in both observed and simulated phytoplankton distributions.

layer nutrient availability driven by variations of the mixed layer (Machu et al., 2005). In austral winter, surface cooling generates a deeper mixing, bringing upward deep nutrient-rich waters, which stimulates plankton production. In the Somalian upwelling region (north of 6°S), high chlorophyll concentrations are more extensive during austral winter. In the subtropical gyre (i.e. offshore of Madagascar), chlorophyll concentrations are low in the model, in line with *SeaWiFS* observations. Although the model is able to reproduce the seasonal variability of the chlorophyll concentration, it fails to reproduce the higher concentrations along the coast, as well as the phytoplankton plume which is noticeable south-east of Madagascar in austral summer (Longhurst, 2001). The weak production along the coast could be related to the absence of a sediment compartment as well as river nutrient discharges in the model simulation. Both resuspension from sediments as well as river discharges enrich the coastal waters with nutrients, enhancing coastal productivity (Lohrenz et al., 1997; Johnson et al., 1999; Booth et al., 2000). The seasonal phytoplankton plume south-east of Madagascar has been recently related to nitrogen fixers (Srokosz and Quartly, 2013), which are not explicitly accounted in for the phytoplankton formulation used in the model.

The effect of mesoscale dynamics on plankton production is summarized in the annual mean primary production presented in Fig. 5. In *NoADV*, the productivity is more localized and confined to coastal regions of the Channel (Fig. 5b). In the presence of eddies in *REF*, coastal productive waters are diffused further offshore (Fig. 5a). The differences in primary production calculated as *REF−NoADV* are positive along the north coast of Mozambique (between 16°S and 10°S),

the central west coast (between 21°S and 17°S) and at the southern tip of Madagascar (Fig. 5c). This is in contrast to reduced primary production in *REF* along the central Mozambican coast (between 25°S and 17°S) and south west of Madagascar (between 26°S and 23°S, Fig. 5c). Offshore in the Mozambique Channel, patterns are more homogeneous with generally increased surface primary production in the simulation with eddies. The vertical structure of primary production shows deeper and weaker subsurface maxima in *NoADV* (Fig. 5e). The shallower subsurface maxima in *REF* suggests an increase of upper layer nutrients induced by eddy dynamics (Fig. 5d).

To interpret these patterns, we examined the changes in nitrate (Fig. 6a–c), which has been suggested to be the limiting factor for phytoplankton production in the Mozambique Channel (Koné et al., 2009). In the northern Mozambique Channel (between 12–17°S), *REF* displays reduced surface nitrate concentrations compared to *NoADV*. This reduced surface nitrate concentration is in contrast to the patterns of productivity presented in Fig. 5c. Phytoplankton growth limitation by nitrate however, follows the production pattern (Fig. 6d–f). It shows that phytoplankton cells are less limited by nitrate in the west side of the basin compared to the east side in *REF* (Fig. 6d). The eddy-driven nitrate transport show a relation with the enhanced production in the west and reduced production in the east side of the basin (Fig. 7a,b). It shows elevated nitrate supply from the north-western side of the basin in *REF* (Fig. 7a), coinciding with the Mozambique Channel eddies main pathway (Halo et al., 2014). In the east side, the eddy-driven nitrate transport is weak and mainly northward. This northward transport is linked to the anticyclonic
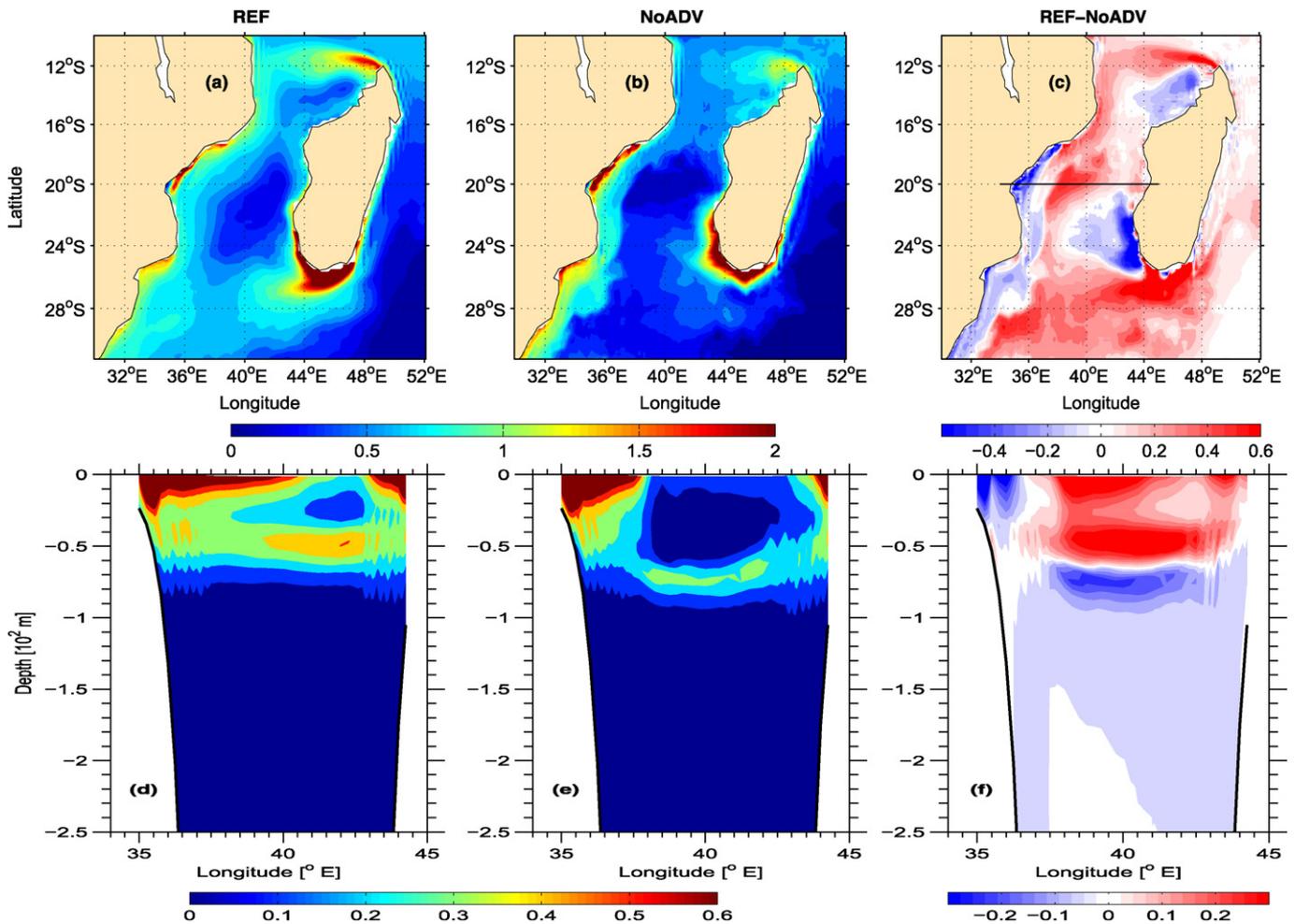
Fig. 5. Surface (a–c) and vertical (d–f) distribution of primary production [mmol C · m^{-3} · d^{-1}], corresponding to *REF* (left panels), *NoADV* (middle column) and the *REF–NoADV* anomalies (right panels). The black line in panel (c) shows the location of the section shown on Fig. 8 and panels d,f.

eddy characteristic of the northern Channel (Collins et al., 2014), which brings less productive waters from the central Channel. In *NoADV*, there is a strong southward transport of nitrate in the northeast side of the basin (Fig. 7b), which explains the enhanced plankton production in Fig. 5c.

Considering now the central Mozambique Channel, the reduction in coastal nitrate south of 17°S (Fig. 6a) is directly related to lateral transport driven by the mesoscale activity (Fig. 7c–d). Eddy dynamics appear to intensify the offshore transport of shelf waters. This offshore transport reduces the nitrate availability in the shelf. In consequence, coastal phytoplankton growth is strongly limited by nitrate (Fig. 6d,e). Further, the eddy-induced lateral nitrate transport increases the offshore nutrient availability, stimulating offshore plankton production, but it is also associated with a reduction in coastal plankton production. These results are in agreement with Gruber et al. (2011) for the California upwelling system, where the authors found a reduction in coastal production caused by eddies.

Another remarkable change associated with advection of momentum is observed on the southern Madagascar shelf. South of Madagascar, the advection of momentum causes a detachment of the *EMC* from the shelf around 45°E (Fig. 1g). A current driven upwelling is associated with the divergence caused by the detachment at the southern tip of Madagascar (Machu et al., 2002). With the cancellation of advection of momentum (i.e. inertia) in *NoADV*, the

EMC hugs the shelf break (Fig. 1h). The coastal upwelling is reduced (Fig. 7f). This can be seen for both primary production and nitrate south of Madagascar (Figs. 5b and 6b). In *REF*, the upwelling along the southern Madagascar coast is intense (Fig. 7e). Even though there is relatively strong upwelling off the south-west coast (between 25°S and 21°S, Fig. 7e,f), the detachment of the *EMC* caused a reduction in surface nitrate availability and phytoplankton production. In *NoADV*, the *EMC* follows the topography and advects nutrients onto the southwestern shelf of Madagascar resulting here in elevated new production when compared to *REF*.

In the central Mozambique Channel at 20°S, the presence of eddies changes the vertical structure of nitrate concentrations Fig. 8ac). The eddy-induced lateral as well as upward transport of nitrate-rich deep waters (Fig. 8d) increases the upper layer nutrient concentrations and shoals the nutricline (Fig. 8a). Thus, phytoplankton growth is enhanced offshore by eddy activity (Fig. 5d–f). The increase of upper layer nutrients and primary production, as well as the favorable light conditions, results in an intensification and shoaling of the subsurface production (Fig. 5d–f). The auto-shading effect (reduction of deep penetration of light due to increased surface production) is also intensified. This can be seen from the vertical distribution of photosynthetically available radiation (*PAR*, Fig. 8f–h). The *PAR* is more attenuated in *REF* (Fig. 8f) than in *NoADV* (Fig. 8g) simulation. This auto-shading effect reduces phytoplankton production below the subsurface maximum (Fig. 5d–f).
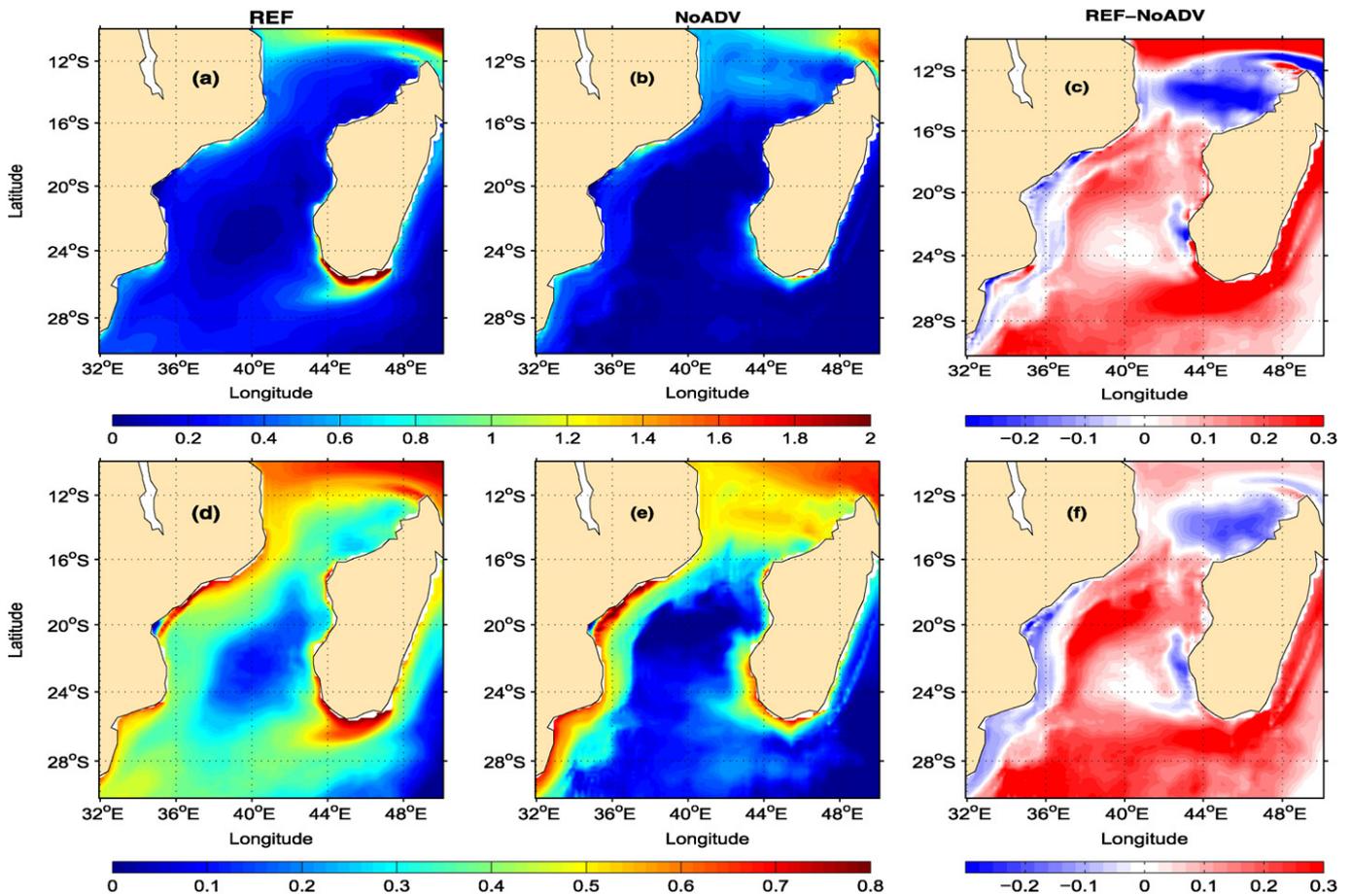
Fig. 6. (a–c) Surface distribution of nitrate [μmol·L^{-1}] in the upper 50 m depth, corresponding to the *REF* simulation and the *REF–NoADV* anomaly. (d–f) The same as (a–c), but for Surface distribution of nanophytoplankton growth limitation by nitrate. Phytoplankton is limited by nitrate when values are below 0.5. For the limitation, we focus our analysis on nanophytoplankton because they represent the most abundant plankton community in this region (Sá et al., 2013).

4. Discussion

The aim of this study is to understand the role of mesoscale dynamics on the phytoplankton production in the Mozambique Channel, known for its strong eddy activity. We approached this task by implementing an idealized experiment in which the processes responsible for small scale generation are removed from the momentum equations. Both mean patterns and turbulent fluxes of this experiment are compared to an eddy-resolving realistic simulation. The cancellation of the non-linear terms did not affect the mean large scale circulation outside the Mozambique Channel (Fig. 1g,h). In the Channel, the mean circulation appear strongly modified by mesoscale dynamics, emphasizing the strong role played by eddy activity on the flow of the Mozambique Channel (Grundlingh, 1995; de Ruijter et al., 2002; Schouten et al., 2003). To the north, the results suggest that the anticyclonic recirculation characteristic of this region (Collins et al., 2014) shape the circulation patterns, by inducing a northward flow on the east side of the basin. This northward flow allows a northward transport of warmer and saltier waters from the central Channel (Fig. 3). These waters are mixed with the relatively cooler and fresher *TSW* brought into the Channel by the *SEC* (Schott and McCreary (2001)). Further south, the *TSW* are diffused offshore by the eddy stirring, reducing the northward propagation of cold southern waters. During this process, waters inshore got saltier and colder while waters offshore got fresher and warmer (Fig. 3).

The changes in the circulation and water mass properties lead to changes in the phytoplankton productivity. It came into view that the eddies in the Mozambique Channel could induce both a reduction and an increase of coastal production (Fig. 5a,b). The reduction of coastal production (which occurs in the central-west and south-east Mozambique Channel) is related to the eddy-induced off-shelf transport of coastal-productive waters, which reduces the coastal nutrient (Fig. 7c,d). With limited nutrients, the phytoplankton growth is reduced due to nutrient-stress (Fig. 6d,e), thus the productivity (Fig. 5c). A similar relationship has been described by Gruber et al. (2011) and Lathuilière et al. (2010) in the eastern tropical upwelling systems. The increased coastal production (which occurs in the northern Channel, Fig. 5a) is related to the eddy-induced nutrient injection into the *MLD* (Fig. 7a,b), as they intensify the southward flow through the Channel (Fig. 2c,d). Vertically, the eddy-induced upward transport of nutrient-rich deep waters (Fig. 8d) combined with eddy-induced lateral transport (Fig. 7a,c) increases the upper layer nutrient concentration (Fig. 8a). This is in agreement with the study by (Oschlies and Garçon, 1998), in which they found about one-third of the total flux of nitrate into the euphotic zone related to eddy activity.

5. Conclusions

It has been shown that eddy activity exerts a suppressive effect on coastal production in eastern boundary upwelling systems, by
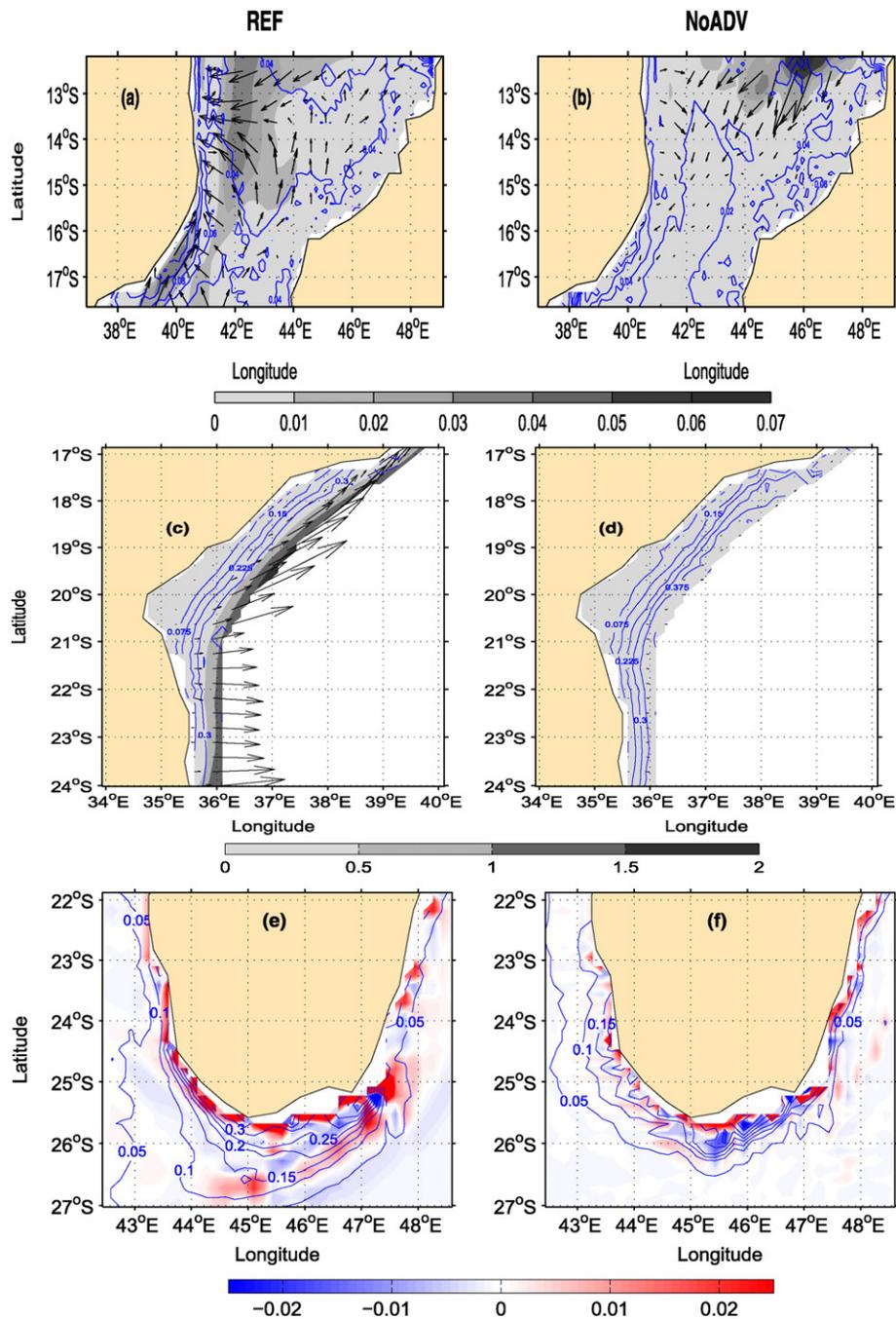
Fig. 7. (a,b) New production (contours, [kmol · s^{-1}]) overlaid on intensity (colour) and direction (arrows) of eddy-driven lateral nitrate transport [kmol N · s^{-1}] integrated over the first 50 m in the northern Mozambique Channel. (c,d) The same as (a,b) but for the coastal domain of the central Mozambique Channel integrated from top to bottom. (e,f) New production integrated over the first 50 m (contours, [kmol · s^{-1}]) overlaid over the mean vertical nitrate transport [kmol N · s^{-1}] accross 50 m depth in the southern Madagascar region. *REF* (left) and *NoADV* (right) simulations. Eddy-driven transport are obtained using the Reynolds decomposition method.

intensifying the lateral transport of nutrient-rich coastal waters (Lathuilière et al., 2010; Gruber et al., 2011). Gruber et al. (2011) have subsequently suggested that a similar effect might occur in other regions characterized by strong eddy activity. Our study on the Mozambique Channel, a region strongly dominated by eddy activity, showed heterogeneous and complex biological responses to eddy activity, with different processes involved in the induced changes. In this region, the mesoscale dynamics have both suppressive, as documented in eastern boundary systems by Gruber et al. (2011), and enhancing effects close to the shore. The suppressive effect was related to eddy-induced offshore transport of coastal nutrients

combined with a reduction in nutrient injection from the lateral boundaries.

The enhancing effect was linked to the intensification of the southward transport of nutrient-rich waters throughtout the northern boundary of the Mozambique Channel. On this basis, it is evident that the role of small-scale dynamics in the marine ecosystem is complex. Their effects on biological production are diverse. This complexity is strongly dependent on the circulation patterns at regional scales, which override the applicability of general schemes. Furthermore, this study emphasizes the need for a good representation of regional circulation patterns in global scale physical
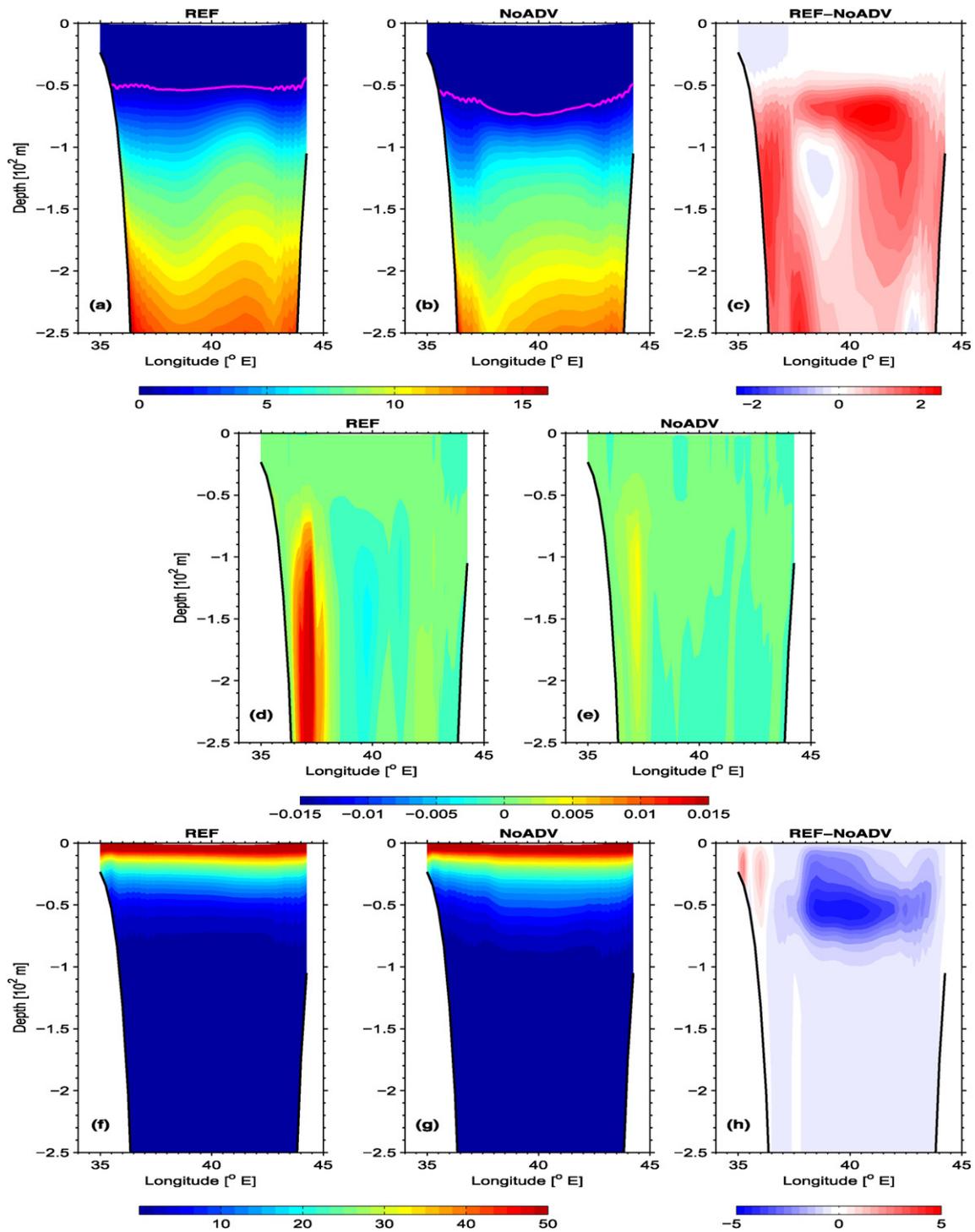
Fig. 8. Vertical structure of: (a–c) nitrate concentration [μmol N $\cdot$ l^{-1}], (d,e) eddy-driven nitrate fluxes [kmol N $\cdot$ s^{-1}] and (f–h) photosynthetic available radiation [W $\cdot$ m^{-2}], along 20°S (section location shown in Fig 5c). D *REF* simulation (a,d,f), *NoADV* simulation (b,e,g) and *REF–NoADV* anomalies (c,h). Eddy-driven transport are obtained using the Reynolds decomposition method.

models to better understand and predict future changes in ocean biogeochemical dynamics.

References

Aumont, O., Bopp, L., 2006. Globalizing results from ocean in situ iron fertilization studies. Glob. Biogeochem. Cycles 20, 1–15. http://dx.doi.org/10.1029/2005GB002591.

Backeberg, B.C., Reason, C.J.C., 2010. A connection between the South Equatorial Current north of Madagascar and Mozambique Channel Eddies. Geophys. Res. Lett. 37, 1–6. http://dx.doi.org/10.1029/2009GL041950.

Booth, J.G., Miller, R.L., McKee, B.A., Leathers, R.A., 2000. Wind-induced bottom sediment resuspension in a microtidal coastal environment. Cont. Shelf Res. 20, 785–806.

Chelton, D.B., deSzoeke, R.A., Schlax, M.G., Naggar, K.E.l., Siwertz, N., 1998. Geographical variability of the first-baroclinic rossby radius of deformation. J. Phys. Oceanogr. 27, 186–194.

Chelton, D.B., Schlax, M.G., Samelson, R.M., de Szoeke, R.A., 2007. Global observations of large oceanic eddies. Geophys. Res. Lett. 34, 1–5. http://dx.doi.org/10.1029/2007GL030812.

Collins, C., Hermes, J.C., Reason, C.J.C., 2014. Mesoscale activity in the Comoros Basin from satellite altimetry and a high-resolution ocean circulation model. J. Geophys. Res. 119, 4745–4760. http://dx.doi.org/10.1002/2014JC010008.

de Ruijter, W.P.M., Ridderinkhof, H., Lutjeharms, J.R.E., 2002. Observations of the flow in the Mozambique Channel. Geophys. Res. Lett. 29, 141–143. http://dx.doi.org/10.1029/95JC01985.

de Ruijter, W.P.M., van Aken, H.M., Beier, E.J., Lutjeharms, J.R.E., Matano, R.P., Schouten, M.W., 2004. Eddies and dipoles around South Madagascar: formation, pathways and large-scale impact. Deep Sea Res., Part I 51, 383400 http://dx.doi.org/10.1016/j.dsr.2003.10.011.

Debreu, L., Marchesiello, P., Penven, P., Cambon, G., 2012. Two-way nesting in split-explicit ocean models: algorithms, implementation and validation. Ocean Model. 49-50, 1–21. http://dx.doi.org/10.1016/j.ocemod.2012.03.003.

Debreu, L., Vouland, C., Blayo, E., 2008. AGRIF: Adaptive grid refinement in fortran. Comput. Geosci. 34, 8–13. http://dx.doi.org/10.1016/j.cageo.2007.01.009.

Eyink, G.L., Sreenivasan, K.R., 2006. Onsager and the theory of hydrodynamic turbulence. Rev. Mod. Phys. 78, 87–135. http://dx.doi.org/10.1103/RevModPhys.78.87.

Fung, I., Tegen, I., 1995. Contribution to the atmospheric mineral aerosol load from land surface modification. J. Geophys. Res. 100, 18707–18726. http://dx.doi.org/10.1029/95JD02051.

Gruber, N., Lachkar, Z., Frenzel, H., Marchesiello, P., Munnich, M., McWilliams, L.C., Nagai, T., Plattner, G.K., 2011. Eddy-induced reduction of biological production in eastern boundary upwelling systems. Nat. Geosci. 4, 1–6. http://dx.doi.org/10.1038/NGEO1273.

Grundlingh, M.L., Carter, R.A., Stanton, R.C., 1991. Circulation and water properties of the southwest indian ocean, spring 1987. Prog. Oceanogr. 28, 305–342.

Grundlingh, M.L., 1995. Tracking eddies in the southeast Atlantic and southwest Indian oceans with TOPEX/POSEIDON. J. Geophys. Res. 100, 24977–24986. http://dx.doi.org/10.1029/95JC01985.

Halo, I., Backeberg, B., Penven, P., Reason, C., Ansorge, I., Ulgren, J., 2014. Eddy properties in the Mozambique Channel: a comparison between satellite altimetry and ocean circulation models. Deep Sea Res., Part II 100, 119–135. http://dx.doi.org/10.1016/j.dsr2.2013.10.015.

Johnson, K.S., Chavez, F.P., Friederich, G.E., 1999. Continental-shelf sediment as a primary source of iron for coastal phytoplankton. Lett. Nature 398, 697–700.

José, Y.S., Mesoscale Structuring of the Pelagic Ecosystem in the Mozambique Channel: A Modelling Approach. Univ. of cape Town

José, Y.S., Aumont, O., Machu, E., Penven, P., Moloney, C.L., Maury, O., 2014. Influence of mesoscale eddies on biological production in the Mozambique Channel: several contrasted examples from a coupled ocean-biogeochemistry model. Deep Sea Res., Part II 100, 79–93. http://dx.doi.org/10.1016/j.dsr2.2013.10.018.

Koné, V., Aumont, O., Lévy, M., Resplandy, L., 2009. Physical and biogeochemical controls of the phytoplankton seasonal cycle in the Indian Ocean: a modelling study. Geophysical Monograph Series 23, 147–166. http://dx.doi.org/10.1029/2008GM000700.

Lathuilière, C., Echevin, V., Lévy, M., Madec, G., 2010. On the role of the mesoscale circulation on an idealized coastal upwelling ecosystem. J. Geophys. Res. 115, 1–14. http://dx.doi.org/10.1029/2009JC005827.

Lebourges-Dhaussy, A., Huggett, J., Ockhuis, S., Roudaut, G., Josse, E., Verheye, H., 2014. Zooplankton size and distribution within mesoscale structures in the Mozambique Channel: a comparative approach using the TAPS acoustic profiler, a multiple net sampler and ZooScan image analysis. Deep Sea Res., Part II 100, 136–152. http://dx.doi.org/10.1016/j.dsr2.2013.10.022.

Lévy, M., Klein, P., Treguier, A.M., 2001. Impact of sub-mesoscale physics on production and subduction of phytoplankton in an oligotrophic regime. J. Mar. Res. 59, 535–565.

Lohrenz, S.E., Fahnenstiel, G.L., Redalje, D.G., Lang, G.A., Chen, X., Dagg, M.J., 1997. Variations in primary production of northern gulf of mexico continental shelf waters linked to nutrient inputs from the Mississippi river. Marine Ecology Progress Series 155. , pp. 45–54.

Longhurst, A., 2001. A major seasonal phytoplankton bloom in the Madagascar basin. Deep Sea Res., Part I 48, 2413–2422. http://dx.doi.org/10.1016/S0967-0637(01)00024-3.

Machu, E., Biastoch, A., Oschlies, A., Kawamiya, M., Lutjeharms, J.R.E., Garçon, V., 2005. Phytoplankton distribution in the Agulhas system from a coupled physical-biological model. Deep Sea Res., Part I 52, 1300–1318. http://dx.doi.org/10.1016/j.dsr.2004.12.008.

Machu, E., Lutjeharms, J.R.E., Webb, A.M., van Aken, H.M., 2002. First hydrographic evidence of the southeast Madagascar upwelling cell. J. Geophys. Res. 29, 1–5. http://dx.doi.org/10.1029/2002GL015381.

McGillicuddy, D., Robinson, A.R., Siegel, D.A., Jannasch, H.W., Johnson, R., Dickey, T.D., McNeil, J., Michaels, A.F., Knap, A.H., 1998. Influence of mesoscale eddies on new production in the Sargasso Sea. Nature 394, 263–266.

New, A.L., Magalhaes, J.M., da Silva, J.C.B., 2013. Internal solitary waves on the Saya de Malha Bank of the Mascarene Plateau: SAR observations and interpretation. Deep Sea Res., Part I 79, 50–61. http://dx.doi.org/10.1016/j.dsr.2013.05.008.

Oschlies, A., Garçon, V., 1998. Eddy-induced enhancement of primary production in a model of the North Atlantic Ocean. Nature 394, 266–269.

Palastanga, V., van Leeuwen, P.J., de Ruijter, W.P.M., 2006. A link between low-frequency mesoscale eddy variability around Madagascar and the large-scale Indian Ocean variability. J. Geophys. Res. 111, 1–15. http://dx.doi.org/10.1029/2005JC003081.

Palastanga, V., van Leeuwen, P.J., Schouten, M.W., de Ruijter, W.P.M., 2007. Flow structure and variability in the Subtropical Indian Ocean: instability of the South Indian Ocean Countercurrent. Prog. Oceanogr. 112, 1–11. http://dx.doi.org/10.1029/2005JC003395.

Penven, P., Marchesiello, P., Debreu, L., Lefevre, L., 2008. Software tools for pre- and post-processing of oceanic regional simulations. Environ. Model. Softw. 23, 660–662. http://dx.doi.org/10.1016/j.envsoft.2007.07.004.

Quartly, G.D., Srokosz, M.A., 2003. A Plankton Guide to Ocean Physics: Colouring in the Currents Around South Africa and Madagascar. 12. The Challenger Society for Marine Science, pp. 19–21.

André, E., Sá, C., Leal, M.C., Silva, A., Nordez, S., Paula, J., Brotas, V., 2013. Variation of phytoplankton assemblages along the Mozambique Coast as revealed by HPLC and microscopy. J. Sea Res. 79, 1–11. http://dx.doi.org/10.1016/j.seares.2013.01.001.

Saetre, R., 1985. Surface currents in the Mozambique Channel. Deep-Sea Res. 32, 1457–1467.

Saetre, R., Silva, A.J.D.a., 1984. The circulation of the Mozambique Channel. Deep Sea Res. Part A 31, 485–508. http://dx.doi.org/10.1016/0198-0149(84)90098-0.

Schott, A.M., Dengler, M., Schoenefeldt, R., 2002. The shallow overturning circulation of the Indian Ocean. Prog. Oceanogr. 53, 57–103. http://dx.doi.org/10.1016/S0079-6611(02)00039-3.

Schott, A.M., McCreary, J.P., 2001. The monsoon circulation of the Indian Ocean. Prog. Oceanogr. 51, 1–123. http://dx.doi.org/10.1016/S0079-6611(01)00083-0.

Schouten, M.W., de Ruijter, A.P.M., van Leeuwen, P.J., Ridderinkhof, H., 2003. Eddies and variability in the Mozambique Channel. Deep Sea Res. Part II 50, 1987–2003. http://dx.doi.org/10.1016/S0967-0645(03)00042-0.

Shchepetkin, A.F., McWilliams, J.C., 2005. The regional oceanic modeling system (ROMS): a split-explicit, free-surface, topography-following-coordinate oceanic model. Ocean Model. 9, 347–404. http://dx.doi.org/10.1016/j.ocemod.2004.08.002.

Siedler, G., Rouault, M., Biastoch, A., Backeberg, B., Reason, C.J.C., Lutjeharms, J.R.E., 2009. Modes of the southern extension of the East Madagascar Current. J. Geophys. Res. 114, 1–15. http://dx.doi.org/10.1029/2008JC004921.

Srokosz, M.A., Quartly, G.D., 2013. The Madagascar bloom: a serendipitous study. J. Geophys. Res. 118, 14–25. http://dx.doi.org/10.1029/2012JC008339.

Ternon, J.F., Roberts, M.J., Morris, T., Hancke, L., Backeberg, B., 2014. Eddies and variability in the Mozambique Channel. Deep Sea Res., Part II 100, 10–26.

Ullgren, J.E., van Aken, H.M., Ridderinkhof, H., de Ruijter, W.P.M., 2012. The hydrography of the Mozambique Channel from six years of continuous temperature, salinity, and velocity observations. Deep Sea Res., Part I 69, 36–50. http://dx.doi.org/10.1016/j.dsr.2012.07.003.

Williams, R.G., Follows, M.J., 1998. The Ekman transfer of nutrients and maintenance of new production over the North Atlantic. Deep Sea Res., Part I 45, 461–489.

Yeung, P.K., Brasseur, J.G., 1991. The response of isotropic turbulence to isotropic and anisotropic forcing at the large scales. Phys. Fhuids A3, 884–897. http://dx.doi.org/10.1063/1.857966.

Zhou, Y., 1993. Interacting scales and energy transfer in isotropic turbulence. Phys. Fhuids A5, 884–897. http://dx.doi.org/10.1063/1.858764.